DETC2011-48652

VIRTUAL REPAIR: GEOMETRIC RECONSTRUCTION FOR REMANUFACTURING GAS TURBINE BLADES

Cecil Piya[a], J. Michael Wilson[a], Sundar Murugappan[a], Yung Shin[a], Karthik Ramani[a,b]

[a] School of Mechanical Engineering, Purdue University, West Lafayette, IN 47906
[b] School of Electrical Engineering (by courtesy), Purdue University, West Lafayette, IN 47906

ABSTRACT

The usage of Direct Metal Deposition (DMD) technology for repairing defective voids in high-value metallic components is time consuming, since traditional geometric reconstruction methods are not seamlessly connected to the DMD process. Here, we consider the development of a semi-automated geometric algorithm for "virtually" repairing defective voids that appear on gas turbine airfoils after extensive use. Our method produces an accurately reconstructed geometric model that can be used for generating DMD scanning paths, while ensuring both dimensional accuracy and topological consistency required by the airfoil design. This model is constructed by using the Sectional Gauss Map concept to generate a series of Prominent Cross Sections (PCS) along the longitudinal axis of a digitally acquired defective airfoil. The intrinsic geometry of the PCS lying in the non-defective region is then extrapolated across the defective region to fill in the voids. A boolean difference between the original defective model and the final reconstructed model yields a fully parameterized geometric representation of the repair volume. The test results of this method demonstrate the algorithm's robustness and versatility over a wide range of airfoil defects.

KEYWORDS Prominent Cross Sections (PCS), Gas turbine blade remanufacturing, Direct Metal Deposition (DMD)

1 INTRODUCTION

Contemporary aeronautical designs require gas turbines to operate within ever increasing temperature ranges [1]. At such temperatures the thermal barrier coating on the turbine blades (airfoils) erode at an expedited rate, making them vulnerable to the abrasive effects of particles ingested by the gas turbines [2]. Moreover, such temperatures also induce hot corrosions, cracks, creep, and dimensional deviations that further contribute towards the presence of defects on airfoil bodies [3].

Ideally, a defective airfoil should be replaced since it causes a significant drop in gas turbine performance, compromising both safety and efficiency of the aircraft. However, airfoil replacement requires exorbitant financial investments, and is rarely a viable solution [4, 5]. It has been estimated that about 70% of defective airfoils in the first stage and 97% of those in the fourth stage of a gas turbine are amenable to repair as opposed to being replaced [3]. Consequently, airfoil defect repair has been a seriously investigated area over the years. It has been projected that conducting airfoil repairs provides a prospect for a 67% increase in financial savings over airfoil replacement [6]. Moreover, reuse of existing airfoils also conforms to the growing practice of sustainable manufacturing.

Most airfoil defects deemed repairable manifest themselves as voids and eroded volumes on the airfoil body [2, 3], and their repair entails an additive remanufacturing process. Traditionally, filler material is added over such voids and is manually welded to the airfoil body [7]. However, with the emergence of the laser based Direct Metal Deposition (DMD) technology, the feasibility of automatically adding material into the voids has grown stronger [6]. The DMD process first injects a stream of powdered material (resembling that of the airfoil) over the defective void, and uses a laser beam to melt and fuse the material with the airfoil body. The path traced by the laser beam is regulated through Computer Numeric Controls (CNC) and is ideally retained within the geometric and dimensional constraints of the airfoil [8].

To effectively carry out the DMD process, a reference geometric model of the defective region must be available. Because the final finish of the repair needs to meet airfoil topological and dimensional requirements, this model requires high levels of accuracy and a well defined parametric

representation (for accurate DMD scanning path generation). The proposed method utilizes the concept of Sectional Gauss Map to extract Prominent Cross Sections (PCS), which captures the intrinsic geometric information of non-defective regions within an airfoil. The PCS are primarily cross-sectional contours, incrementally distributed along the longitudinal axis of the non defective regions. The PCS extracted through our algorithm are transferred into a 3D CAD modeling software, CATIA™ V5, to reconstruct a "virtually" repaired airfoil model by extrapolating the existing geometric information across the defective region. This is followed by registering the orientation of the reconstructed model to that of the original defective model to perform a boolean operation for obtaining a parameterized geometric representation of the repair volume.

2   RELATED WORK AND CONTRIBUTIONS

For several decades Gas Tungsten Arc Welding (GTAW) has been the primary method used for carrying out the additive remanufacturing process [9]. GTAW is limited in terms of the small range of materials it can deal with and the poor strength of bonding it provides between the weld and the damaged part [10]. There have been significant developments made in GTAW to improve its final weld quality and geometric adaptability [11]. However, since this is a manually implemented process, the quality of the final finish of the repair is inconsistent and highly contingent upon the skill of the welder. Even though robot welding systems have been implemented to provide this process with certain level of automation, the welds still exhibit residual stresses induced by high Heat Affected Zones (HAZ). Furthermore, this process is incompatible with the repair of airfoils arranged in a blisk configuration, since there is often inadequate space to fit a welder between the blades [12].

To facilitate the transition into a DMD based repair process, there have been several attempts made towards generating accurate geometric models that assist in DMD scanning path generation. The methods in [7], [13] and [14] manually register a reverse engineered defective airfoil model to a nominal CAD model, and perform a boolean operation to isolate the geometry of the repair volume. These methods make the assumption that a nominal CAD model of the airfoil is available, which is not always the case [15].

The methods described in [16], [17], and [18] reconstruct the repair volume by taking into account the most recent geometric attributes of the airfoil. These methods first compare a template model to the digitized model acquired from the airfoil. The template is then updated based on geometrical changes observed in the airfoil, and the repair volume is extracted through a boolean difference between the updated template and the airfoil data. Although effective in their final outcome, these methods are tedious to implement and require extensive manual input during template update. Furthermore, they are rendered ineffectual when a template model is not available.

Recently, there have been efforts made towards developing a reconstructed model that is entirely independent from any form of nominal or template models. The method used in [15] reconstructs a repaired model by fitting a surface that conforms to the airfoil body over the defective region. However, this method fails to take into account twists and contortions along the airfoil body and will result in inaccurate repair volumes for airfoils with complex geometries. Furthermore, fitting surfaces based on digitized data may lead to out of tolerance surfaces [19, 20].

The reconstruction method used in [21] resolves this issue by sweeping a surface across the defective region. The sweep is based on the cross section(s) lying immediately outside the defective region and guided by curves that represent sweep rails. Since airfoil designs are primarily dictated by the cross sectional geometries along the longitudinal axis of the airfoil body, it makes sense that the airfoil reconstruction is based on the airfoil cross sections [22]. However, the efficacy of this method is undermined as it only considers local neighborhood geometry around the defective region. It fails to account for any global cross sectional geometric variations that exist within the airfoil body.

In this paper we propose to utilize our previously developed algorithm to reconstruct a "virtually" repaired model of the defective airfoil. This algorithm uses the Sectional Gauss Map concept to extract Prominent Cross Sections (PCS) from a mesh object. The PCS extracted from a defective airfoil mesh is thus utilized during model reconstruction. With this method we attempt to rectify the limitations of prior works in virtual repair of gas turbine airfoils by making the following contributions:

- Avoiding reliance on a possibly non-existent or inaccurate nominal CAD model.
- Taking into account crucial global geometric information during reconstruction through the application of Sectional Gauss Map based PCS.
- Increasing the level of automation during model reconstruction and reducing the level of skill required for performing the virtual repair.

3   PROMINENT CROSS SECTIONS (PCS)

This section describes the mathematical theory behind PCS and its implementation on mesh objects. *A PCS at a point on the surface of a solid object is a cross-section of the local sweep segment passing through that point* [23]. C1 and C2 represent two PCS in the hyperboloid of Figure 1 at seed points P1 and P2 respectively. Here, both PCS are part of the same sweep segment.
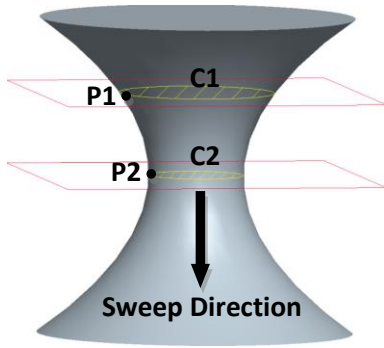
Figure 1: Prominent Cross Sections on a Hyperboloid

3.1 Computing Prominent Cross Sections:

If N is a normal to a surface at point X, then the map $N : X \rightarrow S^2$ transforms this normal to a point on a unit sphere, $S^2 = \{(x, y, z) \in R^3 : x^2 + y^2 + z^2 = 1\}$[24]. This transformation is utilized in the construction of a sectional gauss map while developing a fully optimized PCS.

A fully optimized PCS of a mesh object at a specific seed point lies normal to the local sweep direction at that point, and is obtained through a series of iterative steps. In each iteration, the mesh is first intersected with a cutting plane that passes through the given seed point (cutting plane orientation in first iteration is along a principle curvature direction and the surface normal at the given seed point). The sectional gauss map is then constructed by aligning the pole of a unit sphere with the cutting plane normal, and plotting the normals of the facets intersecting with the cutting plane (N_i) onto the same sphere. This plotting is performed by translating the vectors N_i to the sphere center, and obtaining points where these vectors intersect with the sphere. A least-square fitting is then applied on the plotted points to obtain a new plane, whose orientation is closer to that of the idealized cutting plane at the given seed point. This orientation is then applied to the cutting plane of the ensuing iterative step.

This process is repeated until the angular difference (error value) between the cutting planes of two consecutive iterations falls below a user-defined threshold. The intersecting curve between the final cutting plane and the mesh model is the required PCS at the given seed point. Figure 3 illustrates this iterative process.
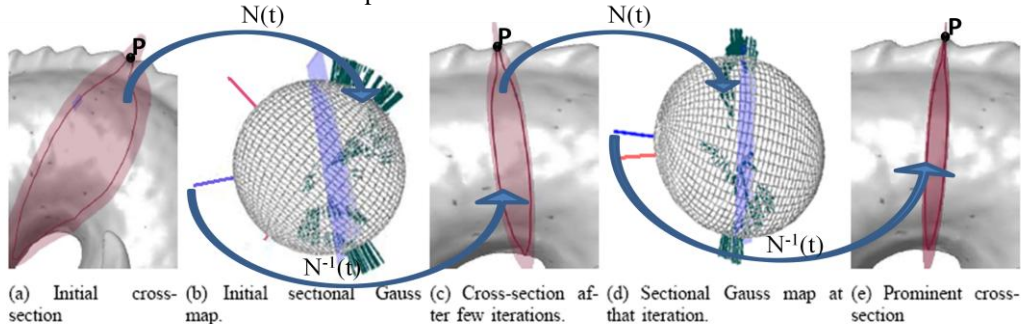
Here, the red and blue lines represent the normal orientations of the initial and final cutting planes within a single iteration. The green lines correspond to the intersecting facet normal vectors, N_i, translated to the sphere center.

3.2 Algorithmic Representation:

Figure 2 provides the pseudo-code for the sectional gauss map algorithm. The following considerations are made during its implementation.

a) The selection of seed points across a meshed object can be manual or automated. In the latter case, uniformly spaced seed points get selected by the k-means algorithm.

b) At each seed point, two PCS are generated: each obtained by orienting the initial cutting plane along a unique principle curvature direction (K_{max} or K_{min}) and the surface normal at the given point. Among the two PCS, the one that yields a lower final error value is retained.

PCS Algorithm *ComputeCrossSections(Mesh)*

for a point p_i ε seed points **do**
    Planes = Identify two starting plane (PI_1 & PI_2) at point (p_i) corresponding to max or min curvature.
    repeat (For each plane PI_i)
        Identify point normals N_i which intersect with (PI_i)
        Plot point normals N_i on Sectional Gauss map
        P_i = Find best fit plane on the Gauss map
    until P_i converges to threshold
    P = Min(error(P_1), error(P_2))
    Generate PCS using P at the point (p_i)
end for

Figure 2: Pseudo-code for Sectional Gauss Map Algorithm [23]

(a) Initial cross-section   (b) Initial sectional Gauss map.   (c) Cross-section after few iterations.   (d) Sectional Gauss map at that iteration.   (e) Prominent cross-section

Figure 3: Optimizing a Cutting Plane at Point P with Sectional Gauss Map

3

4   METHODOLOGY

When represented as a CAD model, the primary geometry of an airfoil is generalized as a single sweep segment. It is imperative that cross sectional curves, incrementally distributed along the sweep direction of the airfoil body, be provided to a CAD modeler while developing this representation. These cross sections ideally lie on planes normal to the sweep direction of the airfoil body. The PCS extracted from the airfoil mesh meet such criteria and serve as quintessential cross sections for the ensuing CAD model. This section describes the use of PCS for virtually reconstructing a defective airfoil and extracting the necessary repair volume.

4.1   Process Pipelines:

There are two pipelines involved in the DMD repair process. Figure 5 shows the primary remanufacturing pipeline. Here, the defects are first pre-machined to provide them with smooth surfaces. This step makes the process of material deposition more convenient as it removes irregular surfaces and sharp inaccessible corners. The DMD process then fills in the pre-machined defects with material. It should be noted that the surface finish of the DMD process contains mild protrusions beyond the specified geometry. As a result, a final surface machining stage is necessary.

Figure 6 illustrates the secondary pipeline which is implemented within the primary pipeline. Here a fully parameterized geometric model required during the DMD process is generated. The details of this pipeline will be described in the ensuing sections.

4.2   Experimental Set-up:

For a preliminary analysis of the proposed methodology, the defective airfoil models used for experimental purposes were created artificially. These models were developed by introducing "virtual defects" into a non defective airfoil model (obtained from an actual physical airfoil) using the CATIA™ V5 CAD system. Nine models with varying levels of defects were created and classified according to defect types: (a) Trailing/Leading Edge Defects, (b) Pressure/Suction Side Defects, and (c) Blade-tip Defects. Few examples of such models are shown in Figure 4.

4.3   PCS Data Extraction and Model Reconstruction:

The PCS in defective airfoil models are generated by implementing the algorithm in Section 3, and visualized through a graphical User Interface (UI) using CGAL [25]. For efficient implementation, the selection of appropriate seed points is done automatically. However, the number of PCS is user specified and based on reconstruction accuracy requirements. Since the primary geometry of the airfoil comprises of only a single sweep component, as opposed to a union of multiple sweep components, the amount of geometric ambiguities that typically result from intersecting volumes is minimal. Consequently, the majority of the PCS generated (about 95%) have been observed to conform to the optimal PCS criteria described in Section 3.
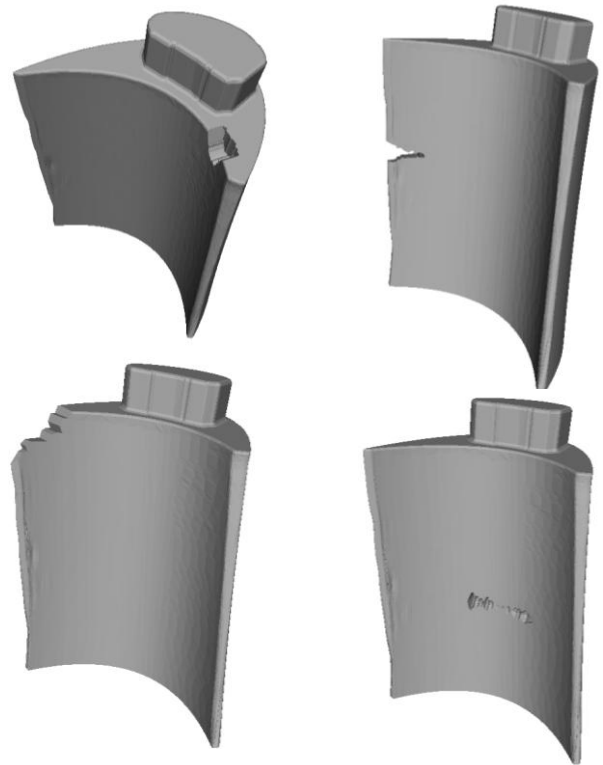

Figure 4: Examples of Defective Airfoil Models created in CATIA™ V5

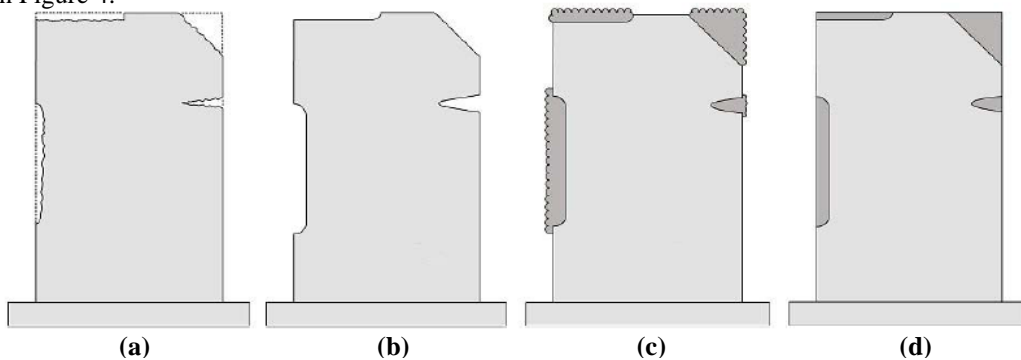| (a) | (b) | (c) | (d) |

Figure 5: Remanufacturing Pipeline: (a) Defective Part, (b) Pre-machined Part, (c) Material Deposited Part, (d) Final Finished Part [16]

The presence of the remaining outlier PCS (about 5%) is a result of geometric and topological inconsistencies resulting from irregular surfaces on the defects of the models. The UI enables manual selection and removal of these outlier PCS. Besides the outliers, the PCS lying over the defective region are also removed, since this region will be reconstructed at a later stage of the pipeline. Figure 6 (b) shows the distribution of PCS over a test model.

The PCS data is exported into CATIA™ as a set of coordinate values of points lying on the PCS. In CATIA™, these points are fitted with interpolation splines (each representing a PCS), and a ruled surface is lofted across the resulting cross-sectional splines (Figure 6(d)). During surface reconstruction, CATIA™ prefers each PCS to have equal number of points, and the points in each PCS to be evenly spaced. To facilitate this, the points in the PCS are subjected to a uniform re-sampling algorithm, [26], that takes into account a user defined PCS point density value.

Figure 7 illustrates the distribution of points on the PCS before and after re-sampling. Besides uniformly distributing points across the PCS, the re-sampling step also aligns the points in adjacent PCS along common iso-parms. As a result, the surface quality and reconstruction rate are significantly improved during model reconstruction.

4.4 Virtual Repair:

Throughout the entire pipeline, the reference coordinate system is kept consistent. Thus, the orientation of the final reconstructed model can be overlapped with that of the original defective model (mesh) in CATIA™ without having to manually register the two. At this stage, a boolean operation between the two models can be performed to extract a geometric model of the repair volume. Since the defective region comprises of irregular surfaces, its exact form cannot be conveniently represented in the model. Therefore, a set of simple planar surfaces that extend slightly beyond the defective region are used to cut out the repair volume.
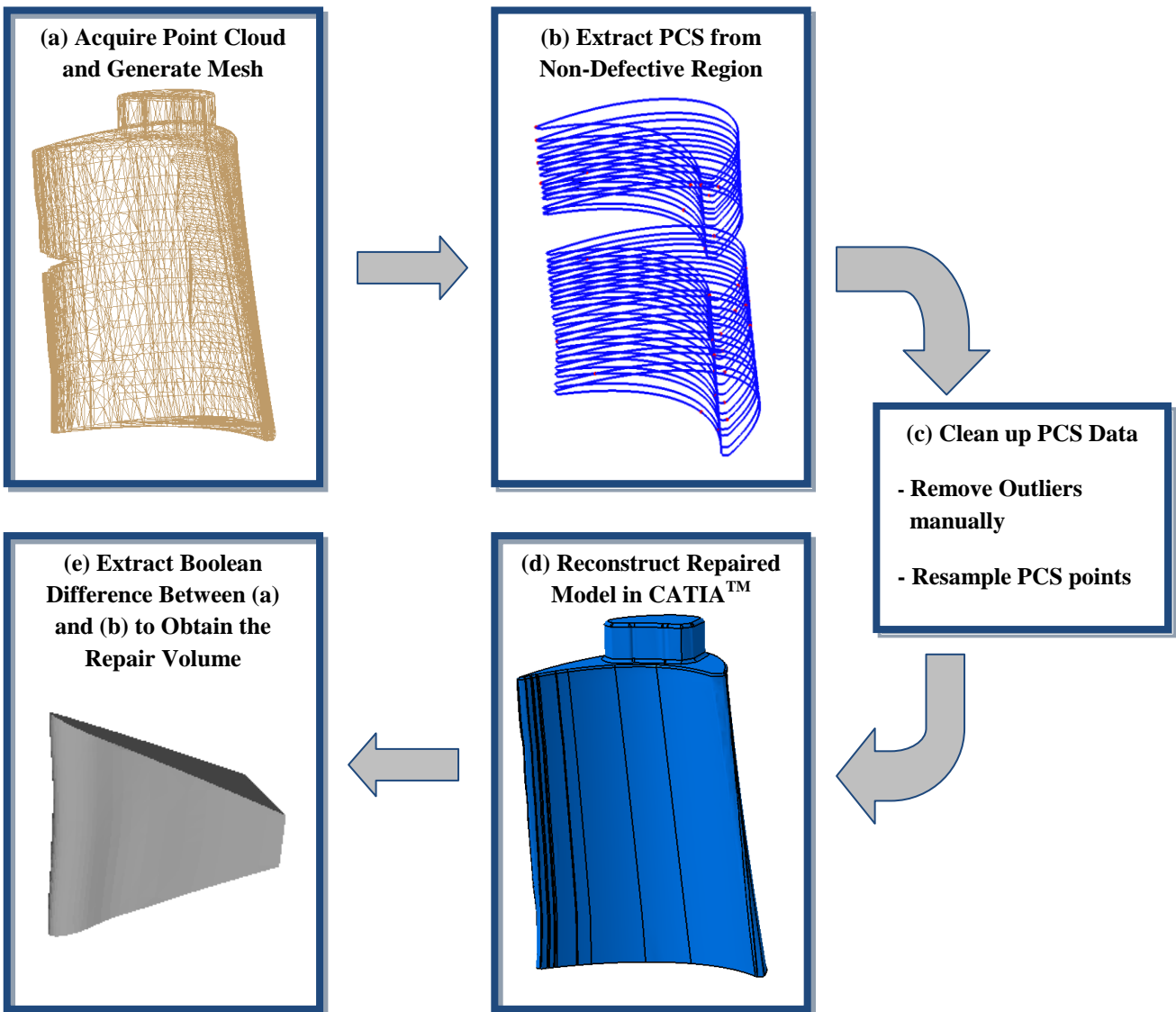

Figure 6: Pipeline for Generating a Parameterized Geometric Model of the Repair Volume
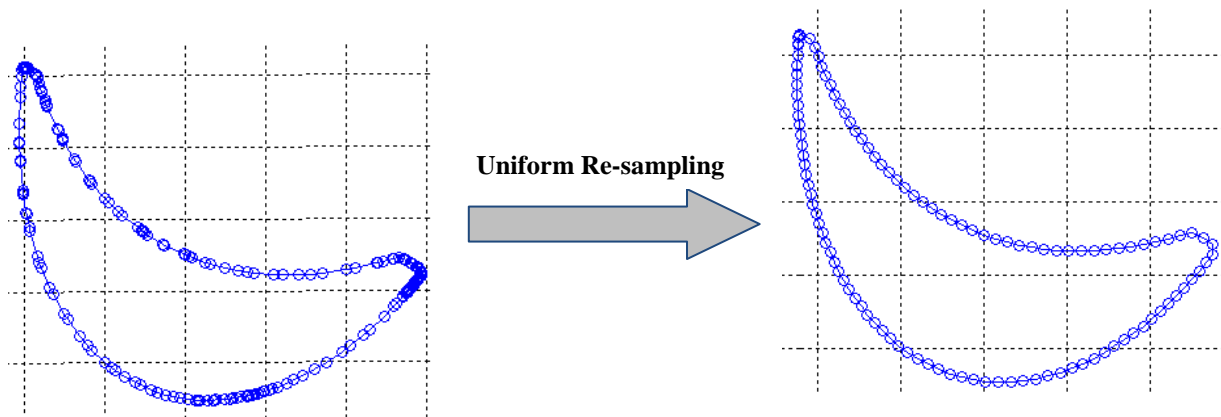
5

Figure 7: Uniform Re-sampling of Points on PCS to Facilitate Surface Reconstruction

The CAD model of the repair volume represents the idealized geometry required for filling in the defective voids in the airfoil without disrupting its overall geometric and topological consistency. This model provides a geometric reference for tool-path generation during the pre-machining and DMD stages of the process pipeline. Since this model is strictly based on the geometric information acquired from the airfoil during digitization and PCS extraction, it does not take into account real world uncertainties associated with the DMD process. Consequently, as mentioned in Section 4.1, the surface finish of the physical repair volume after the DMD process typically exhibits poor surface quality. Therefore, the same idealized virtual model is utilized for generating tool-paths that facilitate the surface finishing process, where the irregular surfaces are leveled to meet surface tolerances.

The repair volume CAD model comprises of two types of surfaces: the surface over the defective region extrapolated from the PCS and the aforementioned planar surfaces used for extracting the repair volume. Since both of these surface types are constructed in CATIA^{TM}, they exist as objects of the CATIA Geometric Modeler (CGM) which provides parametric representations to these surfaces. Such parametric representation of the repair volume model is typically required by CAM software utilized in the DMD and the machining processes for efficient and accurate tool-path generation.

5   RESULTS AND DISCUSSION

This section describes experimental results obtained from the reconstruction tests conducted on the defective airfoil models.

5.1   Reconstruction Accuracy and Build-time:

Figure 8 illustrates the results of a surface error analysis conducted using CATIA^{TM}. Here, the orientation of the original reference model is registered with that of the reconstructed model to determine geometric deviations occurring in the reconstructed model. The color codes indicate the extent of deviation within a specific region. Figure 8(a)

and 8(b) pertain to models whose reconstruction is based on PCS with and without uniformly re-sampled points respectively.
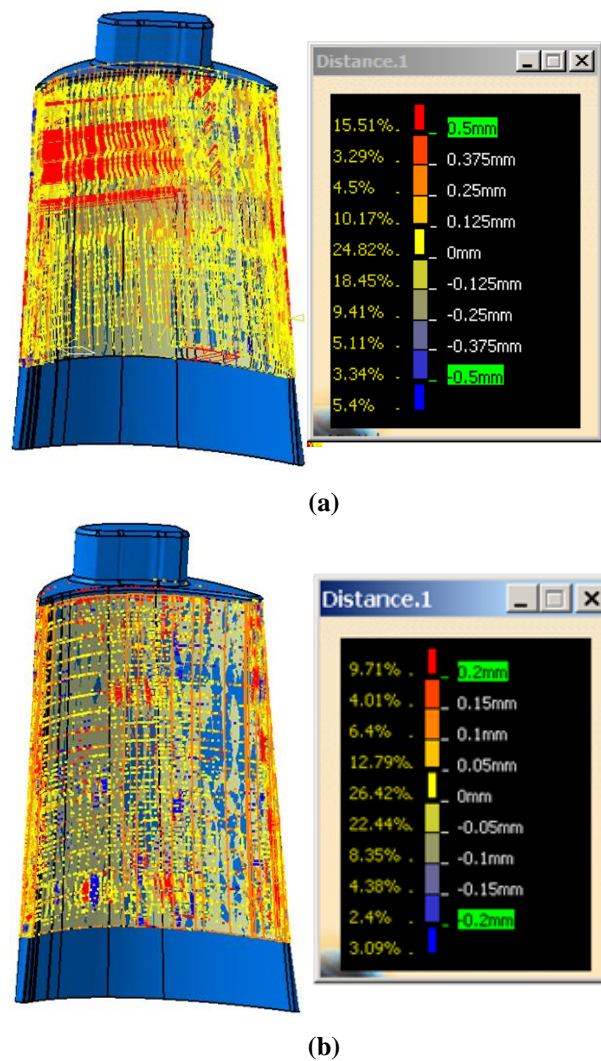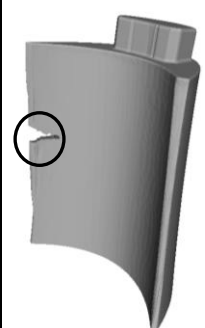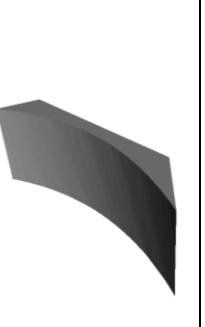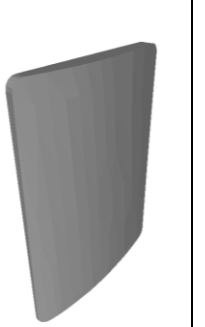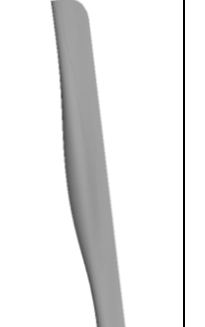

(a)

(b)
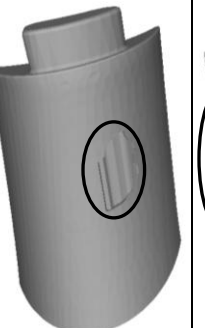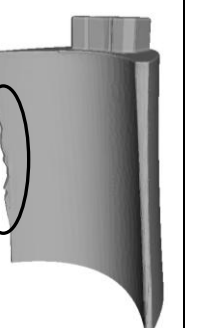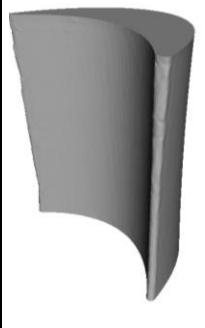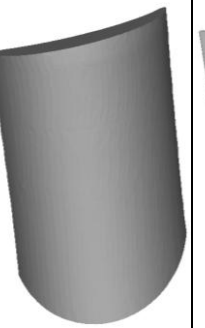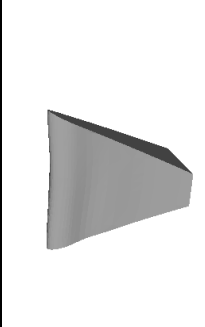
Figure 8: Surface Error Analysis: (a) Model with Uniformly Re-sampled Points on PCS, (b) Model without Re-sampled Points on PCS

6

To determine the geometric deviations, the non defective CAD model mentioned in Section 4.2 (reference model into which "virtual defects" are introduced to obtain defective models) was used as a nominal model against which the virtually repaired models were compared. This comparison was performed with the Distance Analysis tool, which is a part of the Freestyle Shape Workbench in CATIA^{TM}. Basically, this tool first discretises the two models into equal number of elements. It then creates correspondences between the nodes in each model, and finally evaluates distances between corresponding nodes.

It can be seen from Figure 8 that when the PCS points are not subjected to uniform re-sampling, the resulting reconstructed model exhibits lower values of deviations (0.2 mm at most) from the nominal model. However, a lack of organization within the PCS points requires frequent user manipulations during model reconstruction, and thus increases the overall build-time of the reconstructed model. On the contrary, deviations seem to be greater for models reconstructed from PCS with uniformly re-sampled points (up to 0.5 mm). The deviations result from the smoothening effect on PCS curves that occur during uniform re-sampling. However, the build time for the reconstructed model in this case is significantly curtailed, since the organized PCS points accommodate surface lofting criteria (described in Section 4.3) of 3D CAD modeling software and require no user intervention during reconstruction. Therefore, there exists a trade-off between reconstruction accuracy and build-time. This trade-off is contingent upon the extent of automated refinement the PCS points are subjected to. It should be noted that increasing the sampling resolution within the re-sampled PCS can contribute towards reducing the geometric deviations in the final model. However, it can only be achieved at an increased computational cost procured during PCS extraction.

Table 1: "Virtual" Repair on Defective Models and the Extraction of the Repair Volume from the Boolean Operation

	Trailing Edge Defect	Leading Edge Defect	Pressure Side Defect	Suction Side Defect	Trailing Edge Defect
Original Model					
Virtually Repaired Model					
Repair Volume					

5.2 Extraction of Repair Volume:

The first row of Table 1 shows five different defective models used for testing the proposed methodology. The defective regions in those models have been indicated by an ellipse/circle that surrounds the defect. The presence of the defects within an airfoil body is determined based on technical inspections carried out by airfoil maintenance specialists. Since such defective regions are included in the 3D point cloud acquisition process, the irregular surfaces over such regions induce the presence of noise that prevents accurate defect geometry representation in the mesh. However, the exact shape of the defect is irrelevant, since the appropriate geometry of this region will be reconstructed during the virtual repair stage of the pipeline. The only information that is critical is the approximate region over which the defect resides.

The second and third rows of Table 1 illustrate the corresponding "virtually" repaired models and the repair volumes extracted from the defective models in the first row. As mentioned previously in Section 4.4, the repair volumes exist as CAD models whose surfaces are represented in parametric form that facilitates accurate tool path generation. During the physical repair process, the planar surfaces used to cut out the repair volume are used to represent the pre-machined surfaces described in Section 4.1. In the pre-machining stage, all material with irregular surfaces within the defective region and encompassed by these planar surfaces are machined out to make the ensuing DMD process more convenient and feasible.

5.3 Airfoil Tip Defect Repair:

During surface reconstruction, CATIA^{TM} interpolates splines through the PCS points to represent PCS curves. Since the PCS points are sampled from a meshed model, they are not perfectly aligned along smooth curves and cause the interpolated splines to exhibit waviness that is negligible at the local geometric level. For models with defects below the airfoil tip, the reconstruction is bound by PCS at both ends of the defective region (Figure 6(b)). Therefore, the waviness along the surface reconstructed over the defective region remains negligible, since the extrapolation of the PCS curves are consistently constrained. However, for models with tip defects the reconstruction is bound by PCS at only one end of the defective region. Consequently, the PCS splines are extrapolated freely across a specified distance without a 2D geometry constraining the termination point. Such free surface extrapolation causes the waviness in the PCS to get amplified, resulting in reconstructed surfaces that are out of tolerance. It was observed that such erroneous virtual tip defect repairs manifest themselves in two different forms. Figure 9 illustrates the first form in which the reconstructed tip surface directly over the defective region has the presence of a noticeable and

undesirable waviness on it. This wavy reconstructed tip is indicated by the region bounded by the two cross sections at the airfoil tip. The second form is shown in Figure 10, where the resulting repair volume of the tip defect at the leading edge significantly varies from the geometric consistency of the airfoil body, i.e. the leading edge at the reconstructed tip appears abnormally thickened.
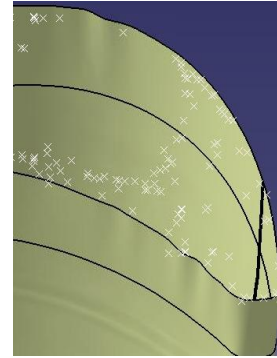

Figure 9: Waviness on Reconstructed Surfaces of Models with Defects at the Airfoil Tip
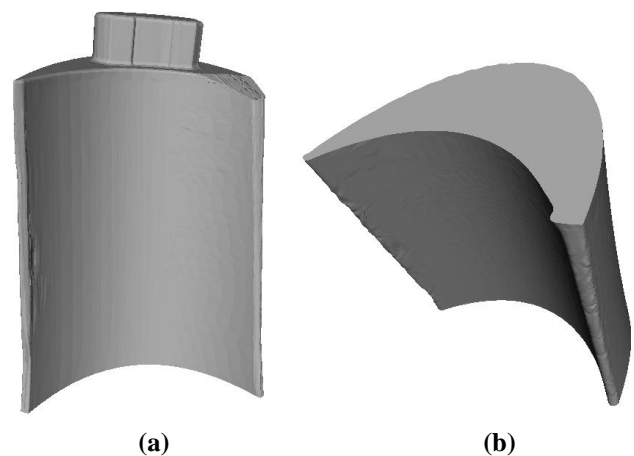

(a)   **(b)**

Figure 10: Erroneous Tip Defect Repair: (a) Model with Leading Edge Tip Defect, (b) Inaccurate Tip Defect Repair

Consequently, it can be concluded that the current method is robust in repairing defects that occur below the airfoil tip, but however needs to include features that will be able to accommodate tip defects as well. Our future works will attempt to accomplish this through the exploration of the following concepts: (a) Moving least square surfaces, (b) Best fit poly-splines (instead of interpolated splines) to represent PCS, and (c) Geometric completion of meshed objects.

6 CONCLUSION

With the development of Direct Metal Deposition (DMD) technologies, the feasibility of gas turbine airfoil repair has significantly increased. To facilitate the DMD based repair process on airfoils with complex geometries, it is

crucial that an accurate geometric representation of the repair volume be available to guide the DMD scanning-paths. This paper proposed a new method for generating such geometric models. Here, the concept of Sectional Gauss Map was used to generate a series of Prominent Cross Sections (PCS) across the longitudinal axis of a defective airfoil mesh. The geometry of the PCS lying within the non-defective regions of the mesh was then extrapolated across the defective region, "virtually" repairing the defect in the process. This method was tested on a variety of defective airfoil models. The results of the experiment indicate that this method is most effective in virtually repairing defects that lie below the tip of the airfoil with a reconstruction error of only $0 - 0.5$ mm.

7   ACKNOWLEDGEMENTS

7   REFERENCES

[1]   Miller, S. "Advanced material mean advanced engines." Materials World [09678638] (1996): 446 -449.

[2]   Grant, G., and Tabakoff, W., "Erosion prediction in turbomachinery resulting from environmental particles," Journal of Aircraft, Vol. 12, No. 5, 1975, pp. 471–478. in Flows Through Cascades," Journal of Aircraft, Vol. 8, No. 1, 1971, pp. 60–64.

[3]   Antony K.C. and Goward, G.W. Aircraft gas turbine blade and vane repair in superalloys , (ed. S. Reichman, D.N. Duhl, G. Maler, S. Antolovich, and C.Lund), 1988, 745-754; Warrendale, PA, The Metallurgical Society.

[4]   Langmaak, S., Scanlan, J. and Wiseall, S. "Design Complexity: a surrogate measure of unit cost", 18 October 2010, URL www.soton.ac.uk/ses/docs/ CEDposters/ CEDposter87.pdf

[5]   Jordal, K, Assadi, M., Genrup, M., "Variations in gas-turbine blade life and cost due to compressor fouling – A Thermoeconomic Approach" Int.J. Applied Thermodynamics,Vol.5, (No.1), pp.37-47, March-2002

[6]   Keicher, D., "Laser engineered net shaping LENS® Phase II." NCMS.org. URL http://technon.ncms.org/ Symposium2005/Presentations/Track%201/0420%20 Keicher.pdf

[7]   Zhend J., Li, Z. and Chen X., "Worn area modeling for automating the repair of turbine blades", The International Journal of Advanced Manufacturing Technology Volume 29, Numbers 9-10, 1062-1067, DOI:10.1007/s00170-003-1990-6

[8]   Karr, S., "Direct metal deposition",URL http:// www. productivitydevelopment.com/92%20Direct%20Metal% 20 Depostion.pdf

[9]   D. L. Keller, D. L. Resor, "Superalloy article cleaning and repair method," U.S. Patent 4,098,540, (1978).

[10]   Eiamsa-ard, K., Janardanan, Nair, H. J., Ren, L., Ruan, J., Sparks, T., and Liou, F. W., "Part repair using a hybrid manufacturing system", Proceedings of the Sixteenth Annual Solid Freeform Fabrication Symposium, Austin, TX, August 1-3, 2005.

[11]   Roy, S., Francoeur, M., "Options forrestoring molds." 25 September 2002.JoiningTechnologies. URL http//:://www.joiningtech.com/publications/moldrestorati on.pdf

[12]   Bonacorso, N., Goncalves, A., and Dutra, J.,"Automation of the processes of surfacemeasurement and of deposition by welding for the recovery of rotors of large-scale hydraulic turbines." Materials Processing Technology (2006): 231-238.

[13]   Brinksmeir E., Berger, U., Jansen, R., "Advanced sensoric and machining system for manufacturing and repair of jet engine components" 31st CIRP international seminar on manufacturing systems, 1998.

[14]   Avagyan V., Zakarian A., Pravansu M. "Scanned three-dimensional model matching and comparison algorithms for manufacturing applications", Journal of Manufacturing Science & Engineering Feb2007, Vol. 129 Issue 1, p190-201

[15]   Gao J., Yilmaz, O., Noble, D., N.Z. Gindy, N., "An integrated adaptive repair solution for complex aerospace components through geometry reconstruction" Int J Adv. Manuf. Technol (2008) 36:1170–1179.

[16]   Bremer C., "Automated repair and overhaul of aero-engine and industrial gas turbine components", Proceedings of the ASME turbo expo 2005, Reno-Tahoe, Nevada, USA, 2005.

[17]   Drechsler, D. E., Cobb, J. N., Humber, M. J. "Method and apparatus for repairing turbine components" United States S.E. Huffman Corp 20080173624 (2008), URLhttp://www.freepatentsonline.com/y2008/0173624. html

[18]   Gao, J., Chen, X., Zheng, D., "Remanufacturing oriented adaptive repair system for worn components," Responsive Manufacturing - Green Manufacturing (ICRM 2010), 5th International Conference,vol., no., pp.11-18, Jan. 2010

[19]   Chen LC, Lin GCI (2000) "Reverse engineering in the design of turbine blades-a case study inapply the MAMDP", Robot Comput-Integr Manuf 16:161–167

[20] Mohaghegh, K., Sadeghi, M.H., Abdullah, A. and Boutorabi, R. "Improvement of reverse engineered turbine blades using construction geometry" The Intern Journal of Adv. Manuf. Tech. Vol. 49, Numbers 5-8, 675-687.

[21] Yilmaz, O., Gindy, N., Gao, J., "A repair and overhaul methodology for aeroengine components", Robotics and Computer Integrated Manufacturing, Volume 26, Issue 2, April 2010, Pages 190-201, ISSN 0736-5845, DOI: 10.1016/j.rcim.2009.07.001.

[22] Liu, Y., Feng, X., Jiang, Z., Dong, X., "High precision modeling of turbine blade from cross section data," Measuring Technology and Mechatronics Automation, International Conference on, pp. 390-393, 2010 International Conference on Measuring Technology and Mechatronics Automation, 2010

[23] Sellamani, S., Muthuganapathy, R., Kalyanaraman, Y., Murugappan, S., Goyal, M., Ramani, K.et. al, "PCS: Prominent cross sections for mesh models", Computer Aided Design and Applications, 7(a), 2010

[24] do Carmo, M.P., "Differential geometry of curves and surfaces", Prentice-Hall (1976). 503 pages

[25] Computational Geometry Algorithms Library, http://www.cgal.org

[26] Wobbrock, J. O., Wilson, A. D., Li, Y., "Gestures without libraires, toolkits or training: A \$1 recognizer for user interface prototypes", UIST '07 Proceedings of the 20th Annual ACM Symposium on User Interface and Software Technology